TAMKANG JOURNAL OF MATHEMATICS
Volume 41, Number 1, 51-69, Spring 2010

ON THE MAXIMAL TEMPORAL AMPLITUDE OF DOWN STREAM RUNNING NONLINEAR WATER WAVES

MARWAN

Abstract. This paper concerns with the down-stream propagation of waves over initially still water. Such a study is relevant to generate waves of large amplitude in wave tanks of a hydrodynamic laboratory. Input in the form of a time signal is provided at the wave-maker located at one side of the wave tank; the resulting wave then propagates over initially still water towards the beach at the other side of the tank. Experiments show that nonlinear effects will deform the wave and may lead to large waves with wave heights larger than twice the original input; the deformations may show itself as peaking and splitting. It is of direct scientific interest to understand and quantify the nonlinear distortion; it is also of much practical interest to know at which location in the wave tank, the extreme position, the waves will achieve their maximum amplitude and to know the amplitude amplification factor. To investigate this, a previously introduced concept called Maximal Temporal Amplitude (MTA) is used: at each location the maximum over time of the wave elevation. An explicit expression of the MTA cannot be found in general from the governing equations and generating signal. In this paper we will use a Korteweg - de Vries (KdV) model and third order approximation theory to calculate the approximate extreme positions for two classes of waves. The classes are the wave-groups that originate from initially bi-chromatics and Benjamin-Feir (BF) type of waves, described by superposition of two or three monochromatic waves. We show that for initially bi-chromatics signals, the extreme position does not depend on the phases of the mono-chromatic components. For BF signals, however, the phases of the mono-chromatic components influence the extreme position essentially. The theoretical results are verified for the case of bi-chromatics with numerical as well as experimental results; for BF signals we use an analytical solution called the Soliton on Finite Background (SFB) for comparison.

1. Introduction

This study is directly motivated to be able to generate extreme waves in wave tanks of hydrodynamic laboratories. In such a generation, a time signal is given to a wave-maker

Received December 18, 2007; revised November 5, 2008.
2000 *Mathematics Subject Classification*. 35Q35, 35Q53, 76B15.
Key words and phrases. Nonlinear distortion, maximal temporal amplitude, modulation instability, bi-chromatics waves, Benjamin-Feir instability, KdV, third order approximation.

that determines the motion of flaps that push the water. Waves are then produced that propagate down stream over initially still water along the wave tank. Because of nonlinear effects the original signal deforms, see [18, 9, 19, 20]. This nonlinear deformation may lead to amplification of the waves so that waves can occur with wave heights that cannot be generated in a direct way by wave-maker motions. The nonlinear effects are difficult to study over the long distances and times that are relevant for the laboratory. In particular it is not clear which waves, i.e. which waves resulting from a certain signal, will show amplitude amplification; and if so, at which position in the tank the largest waves will appear. We will call this position the *extreme position.* The inverse problem, given a specified extreme position, find the possible generating wave-maker signals, is of most scientific interest, and of direct relevance for the hydrodynamic laboratories.

To investigate these problems, it is most fruitful to interpret the down-stream evolution as a spatial succession of wave signals. Directly related to this is a concept called the Maximum Temporal Amplitude (MTA) that has been introduced in [2]. The MTA measures at each location in the wave tank and the wave basin the maximum over time of the surface elevation. The location where the MTA curve achieves its maximum is the extreme position: there the largest waves will be found [13, 14]. The time signal of the surface elevation at that position will be called the extreme signal. Clearly this signal depends on the input at the wave-maker. The ratio of the maximal value of the MTA compared to its value at the wave-maker defines the amplification factor. The MTA can also be used for the inverse problem when a wave-field with a clear extreme position is considered. Suppose that L_D is the distance in the wave tank from the wave-maker where the extreme signal is requested to appear. If the extreme position of the wave-field is denoted by x_{max}, the signal to be generated at the wave-maker should be the the signal of the wave-field at the location of $x = x_{max} - L_D$.

The aim of this paper is to derive the approximate extreme positions for certain wave-fields, and the sensitivity of this position on the phases of constituent monochromatic waves at the wave-maker. We restrict ourselves to wave-fields that arise from bi-chromatics and Benjamin-Feir (BF) wave-maker signals. The bi-chromatics signals consist of two mono-chromatic components of the same amplitudes but slightly different frequencies; the BF signals consist of a large mono-chromatic wave perturbed by two side bands. These signals develop into highly distorted wave-groups with clear amplitude amplification from nonlinear effects. They are prototypes of interesting wave-groups with extreme waves, see for instance the insightful investigations in Longuet-Higgins [12], Phillips [17] and Donelan [7].

For bi-chromatics, many numerical and experimental results are available to verify our theoretical investigation, such as [18, 19]. The BF signals lead to the well known Benjamin Feir instability [5]; this case is particularly nice, since there exists an exact solution of the full nonlinear evolution in the form of an explicit solution of the Nonlinear Schrődinger (NLS) equation called the (spatial) *Soliton on Finite Background* (SFB) [1]. Written in the field variables, see e.g. [4, 10], this spatial SFB is in the far field in the form of a mono-chromatic with two small symmetric side bands, the BF-instability case. For this last case, the amplitude amplification can be as large as three, depending on the modulation length, while for the bi-chromatics it is a bit less.

To simplify the technical calculations in the following, instead of the full surface wave equations, we will use a modified Korteweg - de Vries (KdV) model with exact dispersion relation; for the kind of waves under consideration, this is a valid approximation. As has been shown in previous work, see also [2], for narrow banded spectra, the third order effects can dominate the second order effects and are responsible for the large amplification factors. For that reason we will use third order theory for our analysis.

The organization of the paper is as follows. In the next session we present the mathematical model to be used and the third order asymptotic expansion for this model. In Section 3, we approximate the MTA by an explicit expression obtained from third order theory. In subsection 3.1, we derive the approximate extreme position for bi-chromatics signals, and in subsection 3.2. for BF signals. The effect of the phase of the monochromatic components in the signal at a wave-maker on the extreme position is explicitly presented in the derived formulas. The results, and the verification of the derived formulas for the extreme position are presented in Section 4. Finally in Section 5, we make some concluding remarks.

2. Third order theory for the KdV model

The evolution of rather long and rather small surface gravity waves is governed to a reasonable approximation by the well known KdV equation. In normalized variables, the KdV equation with full dispersion [8] has the form

$$\partial_t \eta + i\Omega(-i\partial_x)\eta + \frac{\mu}{2}\partial_x \eta^2 = 0, \tag{1}$$

where $\eta(x,t)$ is the surface elevation. The parameter μ is the non-linear coefficient, and Ω is the operator that produces the dispersion relation between frequency ω and wave number k for small amplitude waves given by $\omega = \Omega(k) = k\sqrt{\tanh k/k}$.

The laboratory variables for the wave elevation, horizontal space and time η_{lab}, x_{lab}, t_{lab} are related to the normalized variables by $\eta_{lab} = h\eta$, $x_{lab} = hx$ and $t_{lab} = t\sqrt{h/g}$, where h is the uniform water depth and g is the gravity acceleration. Consequently, corresponding transformed wave parameters such as wave length, wave number and angular frequency, are given by $\lambda_{lab} = h\lambda$, $k_{lab} = k/h$, $\omega_{lab} = \omega\sqrt{g/h}$.

In this paper, we approximate solutions of (1) using a direct expansion up to third order in the power series of the wave elevation. Here, we write

$$\eta \approx \varepsilon\eta^{(1)} + \varepsilon^2\eta^{(2)} + \varepsilon^3\eta^{(3)}_{sb}, \tag{2}$$

where ε is a positive small number representing the order of magnitude of the wave amplitude. The terms $\eta^{(1)}, \eta^{(2)}$ and $\eta^{(3)}$ describe the linear first order, the second and third order non-linear term, respectively. Assuming that the linear term $\eta^{(1)}$ consists of three frequencies that are close to each other (narrow band), in the third order we take only the largest contribution, namely the third order side band $\eta^{(3)}_{sb}$. The frequencies of the side bands are close to the frequency of the linear term. It is known that this direct expansion leads to resonance in the third order, see [6, 2]. To prevent the resonant term, we modify this expansion using Linstead-Poincare technique [21] by allowing a nonlinear modification of the dispersion relation

$$k \approx k^{(0)} + \varepsilon k^{(1)} + \varepsilon^2 k^{(2)} \tag{3}$$

with $k^{(0)} = \Omega^{-1}(\omega_0)$.

For the linear signal we take

$$\eta^{(1)} = \sum_{p=1}^{N} a_p e^{i\phi_p} + c.c., \tag{4}$$

where $N = 2$ or 3 for bi-chromatics or BF signals respectively. Here $\phi_p = k_p x - \omega_p t + \psi_p$, where (k_p, ω_p) are related by the linear dispersion relation, and with ψ_p the phase of each mono-chromatic wave; *c.c.* denotes the complex conjugate of the previous terms. The following procedure has been described in [6, 3] without taking the phases of the mono-chromatic components of the signals into account, i.e. for $\psi_p = 0$. Since we aim to investigate the effect of these mono-chromatic phases on the global behaviour of the propagating signal along the wave tank, we add arbitrary phases ψ_p. Substituting (2) and (3) into (1), for $\eta^{(1)}$ as the linearized solution as in (4), the second order leads to $k_p^{(1)} = 0$, $p = 1, \ldots, N$ and

$$\eta^{(2)} = \mu \left(\sum_{p=1}^{N} \sum_{q=1}^{N} a_p a_q \left(s_+ e^{i(\phi_p + \phi_q)} + s_- e^{i(\phi_p - \phi_q)} \right) \right) + c.c., \tag{5}$$

where

$$s_\pm = \frac{1}{2} \frac{k_p^{(0)} \pm k_q^{(0)}}{\omega_p \pm \omega_q - \Omega(k_p^{(0)} \pm k_q^{(0)})}.$$

In order to distinguish the free waves that will be introduced later, we call the second order solution in (5) the second order bound wave; this solution contains non-linear terms as the results of mode generation. The resonant terms in the third order bound wave, lead to the non-linear dispersion relation

$$k_p^{nl} = k_p^{(0)} + k_p^{(2)}$$

with

$$k_p^{(2)} = -\mu^2 \frac{k_p^{(0)}}{V_g(k_p^{(0)})} \left(\sum_{q=1}^{N} a_q^2 (s_+ + s_-) \right), \ p = 1, \ldots, N. \tag{6}$$

The third order side band $\eta_{sb}^{(3)}$ can be expressed as

$$\begin{aligned} \eta_{sb}^{(3)} = {} & \mu^2 \sum_{p=q}^{N} \sum_{q \neq r}^{N} \sum_{r=1}^{N} a_p a_q a_r L_{pq,r} (s_p + s_{q,r}) e^{i(\phi_p + \phi_q - \phi_r)} \\ & + \frac{1}{2} \mu^2 \sum_{p \neq q, p \neq r}^{N} \sum_{q \neq r}^{N} \sum_{r=1}^{N} a_p a_q a_r L_{pq,r} (s_{p,r} + s_{pq} + s_{q,r}) e^{i(\phi_p + \phi_q - \phi_r)} + c.c., \end{aligned} \tag{7}$$

where

$$s_p = \frac{k_p^{(0)}}{2\omega_p - \Omega(2k_p^{(0)})}, \quad s_{pq} = \frac{1}{2}\frac{k_p^{(0)} + k_q^{(0)}}{\omega_p + \omega_q - \Omega(k_p^{(0)} + k_q^{(0)})},$$

$$s_{p,r} = \frac{k_p^{(0)} - k_r^{(0)}}{\omega_p - \omega_r - \Omega(k_p^{(0)} - k_r^{(0)})}, \quad L_{pq,r} = \frac{k_p^{(0)} + k_q^{(0)} - k_r^{(0)}}{\omega_p + \omega_q - \omega_r - \Omega(k_p^{(0)} + k_q^{(0)} - k_r^{(0)})},$$

and

$$V_g(k_p^{(0)}) = \Omega'(k_p^{(0)}), \; p = 1, \ldots, N.$$

In this paper, we mimic the generation of waves in a hydrodynamic laboratory and so we are interested in a solution that at a given position, say $x = 0$, is given by the signal

$$\widetilde{\eta}(0,t) = \sum_{p=1}^{N} a_p e^{i\theta_p} + c.c., \tag{8}$$

where $\theta_p = \omega_p t + \psi_p$, $p = 1, 2, 3$. To satisfy the signal at this position, the contribution of the second order and third order side band terms at $x = 0$ have to be compensated by harmonic modes, called free waves. The second order free waves are given by

$$\eta_{free}^{(2)} = \mu \left[\sum_{p=1}^{N} \sum_{q=1}^{N} a_p a_q \left(s_+ e^{i\vartheta(\omega_p + \omega_q)} + s_- e^{i\vartheta(\omega_p - \omega_q)} \right) \right] + c.c. \tag{9}$$

This is a wave with the same frequencies as in the second order bound wave, but consisting of harmonic modes that satisfy the linear dispersion relation. The third order side band free wave consists similarly of monochromatic waves and is of the form

$$\begin{aligned} \eta_{sb,free}^{(3)} &= \mu^2 \sum_{p=q}^{N} \sum_{q \neq r}^{N} \sum_{r=1}^{N} a_p a_q a_r L_{pq,r} (s_p + s_{q,r}) e^{i\vartheta(\omega_p + \omega_q - \omega_r)} \\ &+ \frac{1}{2}\mu^2 \sum_{p \neq q, p \neq r}^{N} \sum_{q \neq r}^{N} \sum_{r=1}^{N} a_p a_q a_r L_{pq,r} (s_{p,r} + s_{pq} + s_{q,r}) e^{i\vartheta(\omega_p + \omega_q - \omega_r)} + c.c., \end{aligned} \tag{10}$$

with $\vartheta(\omega_p) = \Omega^{-1}(\omega_p)x - \omega_p t + \psi_p$, $p = 1, \ldots, N$. Taken together, the third order solution of (1) and satisfying (8) is

$$\widetilde{\eta} \approx \eta^{(1)} + \eta^{(2)} - \eta_{free}^{(2)} + \eta_{sb}^{(3)} - \eta_{sb,free}^{(3)}. \tag{11}$$

3. Maximal Temporal Amplitude and the extreme position

In previous studies of bi-chromatics waves [18], [9], [19], [20], it was found experimentally, numerically and theoretically that depending on the wave amplitude, but just as well as on the frequency difference, large deformations and amplitude increase can develop. This was made more clearly visible in [2] where, for the corresponding optical problem, the so-called *maximal temporal amplitude* (MTA) was introduced. At each position downstream from the wave generator, this MTA measures the maximum over time of the surface elevation. When plotted as a curve in the down stream direction, this curve shows (almost periodic) oscillatory behaviour in which several wavelengths can be seen and interpreted. At specific locations the curve achieves its maximum at places where the amplitude amplification (compared to the amplitude of the generated wave) is maximal and where 'extreme' waves appear.

According to the previous section, the third order approximated solution of (1)is given by (11); we will use this approximation to study the MTA, and hence we take the MTA to be defined as

$$m(x) = \max_t \widetilde{\eta}(x,t). \tag{12}$$

In deterministic extreme wave generation performed in hydrodynamic laboratories, MTA is proved to be a useful concept to predict the position where the most extreme signal appears in the wave tank, [4]. Furthermore, it gives a practical value of the Amplitude Amplification Factor, AAF $= m(x_{\max})/m(0)$, where $x_{\max}$ is the first position where $m(x_{\max}) = \max_x m(x)$, for $0 < x < L$ and L the length of the wave tank. Therefore it is of interest to calculate the value of $x_{\max}$ and the dependence of this position on the input signal at the wave-maker.

In [2] an explicit expression was given for $x_{\max}$ for input signals in the form of bi-chromatics waves with zero phases for a KdV model of an optical pulse propagation in non-linear media using third order approximation. A similar formulation for uni-directional bi-chromatics are derived in [13] for propagation of water wave where the initial phases of the mono-chromatic components are zero. It will be shown in the next subsection that for bi-chromatics signals $x_{\max}$ does not depend on the initial phases of the mono-chromatic components. In the second subsection we will consider the similar problem for BF-signals.

3.1. The extreme position for bi-chromatics signals

In the following we briefly derive the explicit expression of $x_{\max}$ for an input signal in the form of bi-chromatics wave and show that this $x_{\max}$ does not depend on the initial phases of the mono-chromatic components. Denoting the indices 1 and 2 in the expressions (4) – (10) by $(+)$ and $(-)$ for the case of bi-chromatics signals, the linear term can be written as

$$\eta^{(1)} = q(\cos\theta_+ + \cos\theta_-), \tag{13}$$

where $\theta_\pm = k_\pm^{(0)}x - \omega_\pm t + \psi_\pm$, with $\psi_\pm$ the phase of each mono-chromatic wave, and the wave numbers ordered according to $k_+^{(0)} > k_-^{(0)}$.

The following expressions are rewritten from (5)–(10).

$$\eta^{(2)} = \mu q^2 (s_+ \cos(2\theta_+) + s_- \cos(2\theta_-) + 2s\cos(\theta_+ + \theta_-) + s_0 \cos(\theta_+ - \theta_-)), \tag{14}$$

$$\begin{aligned}\eta_{fw}^{(2)} = \mu q^2 &\left[s_+ \cos(\Omega^{-1}(2\omega_+)x - 2\omega_+ t) + s_- \cos(\Omega^{-1}(2\omega_-)x - 2\omega_- t)\right] \\ &+\mu q^2 \left[2s \cos(\Omega^{-1}(\omega_+ + \omega_-)x - (\omega_+ + \omega_-)t)\right] \\ &+\mu q^2 \left[s_0 \cos(\Omega^{-1}(\omega_+ - \omega_-)x - (\omega_+ - \omega_-)t)\right],\end{aligned} \tag{15}$$

$$k_{\pm}^{(2)} = -\mu^2 q^2 \frac{k_{\pm}^{(0)}}{Vg(k_{\pm}^{(0)})}(s_0 + s_{\pm} + 2s). \tag{16}$$

Using this wave number correction, the first order expansion $\eta^{(1)}$ can be written as

$$\eta^{(1)} = 2q \cos(\overline{k}^{nl} x - \overline{\omega} t + \alpha_+) \cos(\kappa x - \nu t + \alpha_-) \tag{17}$$

with $\overline{\omega} = (\omega_+ + \omega_-)/2,\ \nu = (\omega_+ - \omega_-)/2$ and $\kappa = \Omega^{-1}(\nu)$.

The third order bound and free waves are expressed as

$$\begin{aligned}\eta_{sb}^{(3)} = q^3 B_+ \cos(\overline{k}^{nl} x - \overline{\omega} t + \alpha_+) \cos(3\kappa^{nl} x - 3\nu t + 3\alpha_-) - \\ q^3 B_- \sin(\overline{k}^{nl} x - \overline{\omega} t + \alpha_+) \sin(3\kappa^{nl} x - 3\nu t + 3\alpha_-)\end{aligned} \tag{18}$$

and

$$\begin{aligned}\eta_{sb,fw}^{(3)} = q^3 B_+ \cos(\overline{K} x - \overline{\omega} t + \alpha_+) \cos(\widetilde{K} x - 3\nu t + 3\alpha_-) - \\ q^3 B_- \sin(\overline{K} x - \overline{\omega} t + \alpha_+) \sin(\widetilde{K} x - 3\nu t + 3\alpha_-),\end{aligned} \tag{19}$$

where $\overline{k}^{nl}$ and κ^{nl} are nonlinear wave numbers; corresponding to $\overline{\omega}$ and ν respectively, $\overline{K} = (\Omega^{-1}(2\omega_+ - \omega_-) + \Omega^{-1}(2\omega_- - \omega_+))/2,\ \widetilde{K} = (\Omega^{-1}(2\omega_+ - \omega_-) - \Omega^{-1}(2\omega_- - \omega_+))/2.$ The coefficients of third order side bands are $B_{\pm} = a_+ \pm a_-$, with

$$\begin{aligned}a_+ &= \mu^2 (s_+ + s_0) \frac{2k_+^{(0)} - k_-^{(0)}}{2\omega_+ - \omega_- - \Omega(2k_+^{(0)} - k_-^{(0)})}, \\ a_- &= \mu^2 (s_- + s_0) \frac{2k_-^{(0)} - k_+^{(0)}}{2\omega_- - \omega_+ - \Omega(2k_-^{(0)} - k_+^{(0)})},\end{aligned}$$

see [13], $\alpha_+ = (\psi_+ + \psi_-)/2$, and $\alpha_- = (\psi_+ - \psi_-)/2$.

For wave parameters of laboratory interest $B_- << B_+$, the expressions (17) and (18) show that the first and the third order side band bound wave have approximately the same carrier. The superposition of the first order with the third order side band bound and free waves leads to a spatial envelope of the carrier wave, resulting in a modulation of the carrier. Under the assumption $B_- << B_+$, the phases of first order, third order side band bound and free waves are the same, namely α_+, and so the spatial envelope has modulation length $\lambda = 2\pi / \left|(\overline{k}^{nl} - \overline{K})/2\right|$. This value can in fact be obtained by considering the superposition of the third order bound waves and free waves only where λ appears as the 'wave length' of MTA. The positions of zero phase of the spatial envelope show that the location of the first maximum of MTA does not depend on the phases of mono-chromatic components and it can be expressed in the form

$$
\begin{aligned}
\check{x}_{\max} &\approx \frac{\pi}{\left|\overline{k}^{nl} - \overline{K}\right|} \\
&\approx \frac{\pi}{\left|2\nu^2\tilde{\beta} + 2q^2(\tilde{\gamma} + 2\mu^2\sigma_2\overline{k}/V_g(\overline{k}))\right|} \\
&= \mathcal{O}\left(\frac{1}{\nu^2}, \frac{1}{q^2}\right)
\end{aligned}
\tag{20}
$$

where

$$
\tilde{\beta} = -\frac{\Omega''(\overline{k})}{2V_g^3(\overline{k})}, \quad \tilde{\gamma} = \frac{\mu^2\overline{k}}{V_g(\overline{k})}\left(\frac{1}{V_g(\overline{k}) - 1} + \frac{\overline{k}}{2\overline{\omega} - \Omega(2\overline{k})}\right) \text{ and } \sigma_2 = \frac{\overline{k}}{2\overline{\omega} - \Omega(2\overline{k})}.
$$

3.2. Extreme position for BF signals

Recent progress in deterministic extreme wave generation is based on the so called (spatial) Soliton on Finite Background (SFB), [4, 10, 11]. The SFB is an exact solution of the (spatial) Non-linear Schrodinger equation and is described in detail in [1] and has been considered in [15, 16] as a possible description of large amplitude increase for surface waves, leading to ‘freak’, or ‘rogue’ waves. This spatial SFB is at each position periodic in time, but with surface wave elevations that resemble a soliton profile in space. But the asymptotic values have a finite nonzero value, the amplitude of the mono-chromatic wave in the far field. Written in physical variables, SFB is the nonlinear extension of the modulation (Benjamin-Feir) spatial instability of a mono-chromatic wave. The family of SFB solutions depend essentially on three parameters, namely the frequency of the carrier waves, the modulation length, and the maximum amplitude of the extreme signal; one of these parameters can be replaced by the amplitude of the asymptotic mono-chromatic wave. The first parameter, the frequency of the carrier wave, enters indirectly through the value of the coefficients of the NLS equation.

In the far field the physical SFB is a modulated mono-chromatic wave, a mono-chromatic wave with two symmetric side bands. The frequencies are therefore written as the central frequency $\omega_2 = \omega_0$, and sidebands $\omega_3 = \omega_0 + \nu$, $\omega_1 = \omega_0 - \nu$. The amplitude of the central wave is a_0, and ones of the side bands are $a_3 = a_1 = \delta a_0$ for some small parameter δ. In this paper, we will investigate the effects of the initial phases of the mono-chromatic components. This makes that we take (8) in the form

$$
\widetilde{\eta}(0, t) = a_0 e^{i(-\omega_0 t + \psi_0)} + \delta a_0 e^{i(-\omega_1 t + \psi_1)} + \delta a_0 e^{i(-\omega_3 t + \psi_3)} + c.c. \tag{21}
$$

where ψ_0 and ψ_1, ψ_3 are the initial phases of the mono-chromatic and the two side bands respectively. For ease of presentation, we rewrite the phases ψ_0, ψ_1 and ψ_3 as

$\psi_1 = \psi_0 + \alpha - \beta$ and $\psi_3 = \psi_0 + \alpha + \beta$, with arbitrary values of ψ_0, α and β. Then the expression for the signal at the wave-maker can be written as

$$\begin{aligned}\widetilde{\eta}(0,t) &= a_0 e^{i(-\omega_0 t+\psi_0)} + \delta a_0 e^{i\alpha}[e^{-i(-\nu t+\beta)} + e^{i(-\nu t+\beta)}]e^{i(\omega_0 t+\psi_0)} + c.c. \\ &= a_0[1+2\delta e^{i\alpha}\cos(-\nu t+\beta)]e^{i(-\omega_0 t+\psi_0)} + c.c.\end{aligned} \tag{22}$$

The expression of $\eta^{(1)}(x,t)$ in (4) becomes

$$\begin{aligned}\eta^{(1)}(x,t) &= a_0 e^{i(k_0^{nl}x-\omega_0 t+\psi_0)} + \delta a_0 e^{i(k_1^{nl}x-\omega_1 t+\psi_1)} + \delta a_0 e^{i(k_3^{nl}x-\omega_3 t+\psi_3)} + c.c. \\ &= a_0[1+2\delta e^{i((\overline{k^{nl}}-k_0^{nl})x+\alpha)}\cos(\kappa^{nl}x-\nu t+\beta)]e^{i(k_0^{nl}x-\omega_0 t+\psi_0)} + c.c.\end{aligned} \tag{23}$$

where $\overline{k^{nl}} = (k_1^{nl}+k_3^{nl})/2$, $\kappa^{nl} = (k_3^{nl}-k_1^{nl})/2$, and k_0^{nl} is the non-liner wave number corresponding to ω_0. From (23), we observe that the superposition of the three monochromatic waves leads to a spatial envelope that is modulated with wave length $\lambda_1 = 2\pi/|\overline{k^{nl}}-k_0^{nl}|$.

As shown in [2, 13], the second order terms do not affect the extreme position; hence this position can be approximated by considering the first and the third order side bands only. The most important third order side bands that determine the position are the terms in (7) that have wave numbers close to that of the first order term. These important terms as a part of $\eta_{sb}^{(3)}$ can be written in the form

$$\begin{aligned}\eta_{sb}^{(3)*}(x,t) = {} & a_0^3\rho e^{i((k_3^{nl}+k_1^{nl}-k_0^{nl})x-\omega_0 t+\psi_0+2\alpha)} \\ & + a_0^3\beta_{-3}e^{i((2k_0^{nl}-k_1^{nl})x-(\omega_0-\nu)t+\psi_0-\alpha+\beta)} \\ & + a_0^3\beta_{+3}e^{i((2k_0^{nl}-k_3^{nl})x-(\omega_0+\nu)t+\psi_0-\alpha-\beta)} + c.c.,\end{aligned} \tag{24}$$

and the corresponding terms of $\eta_{sb,free}^{(3)}(x,t)$ are

$$\begin{aligned}\eta_{sb,free}^{(3)*}(x,t) = {} & a_0^3\rho e^{i(\Omega^{-1}(\omega_0)x-\omega_0 t+\psi_0+2\alpha)} \\ & + a_0^3\beta_{-3}e^{i(\Omega^{-1}(2\omega_0-\omega_1)x-(\omega_0-\nu)t+\psi_0-\alpha+\beta)} \\ & + a_0^3\beta_{+3}e^{i(\Omega^{-1}(2\omega_0-\omega_3)x-(\omega_0+\nu)t+\psi_0-\alpha-\beta)} + c.c.\end{aligned} \tag{25}$$

Here $\rho = \delta^2\mu^2(s_{1,2}+s_{3,2}+s_{13})L_{13,2}$, $\beta_{-3} = \delta\mu^2(s_{2,1}+s_2)L_{22,1}$, and $\beta_{+3} = \delta\mu^2(s_{2,3}+s_2)L_{22,3}$. Since $\delta << 1$ it follows that $\rho << \beta_{\pm 3}$ and so the terms $a_0^3\rho\cos((k_3^{nl}+k_1^{nl}-k_0^{nl})x+\psi_0+2\alpha)$ in $\eta_{sb}^{(3)*}(x,t)$ and $a_0^3\rho\cos(\Omega^{-1}(\omega_0)x+\psi_0+2\alpha)$ in $\eta_{sb,free}^{(3)*}(x,t)$ can be neglected. The remaining terms in (24) and (25) become

$$\begin{aligned}\eta_{sb}^{(3)*}(x,t) &\approx a_0^3\beta_{-3}e^{i\{[(k_0^{nl}-\overline{k^{nl}})x-\alpha]+[\kappa^{nl}x-\nu t+\beta]+[k_0^{nl}x-\omega_0 t+\psi_0]\}} \\ &\quad + a_0^3\beta_{+3}e^{i\{[(k_0^{nl}-\overline{k^{nl}})x-\alpha]-[\kappa^{nl}x-\nu t+\beta]+[k_0^{nl}x-\omega_0 t+\psi_0]\}} + c.c. \\ &\approx a_0^3 e^{-i[(\overline{k^{nl}}-k_0^{nl})x+\alpha]}B_{bw}(x,t)e^{i[k_0^{nl}x-\omega_0 t+\psi_0]} + c.c.,\end{aligned} \tag{26}$$

and

$$\eta_{sb,free}^{(3)*}(x,t) \approx a_0^3 e^{-i[-\frac{1}{2}K''(\omega_0)\nu^2 x+\alpha]}B_{fw}(x,t)e^{i[K(\omega_0)x-\omega_0 t+\psi_0]} + c.c., \tag{27}$$

where

$$B_{bw}(x,t) = \beta_{-3}e^{i[\kappa^{nl}x-\nu t+\beta]} + \beta_{+3}e^{-i[\kappa^{nl}x-\nu t+\beta]},$$
$$B_{fw}(x,t) = \beta_{-3}e^{i[K'(\omega_0)\nu x-\nu t+\beta]} + \beta_{+3}e^{-i[K'(\omega_0)\nu x-\nu t+\beta]},$$

$K(\omega_0) = \Omega^{-1}(\omega_0)$, and $K(\omega_0 \pm \nu) \approx K(\omega_0) \pm K'(\omega_0)\nu + K''(\omega_0)\nu^2/2$.

It is interesting to see that the third order side band bound and free waves have spatial envelopes that do not depend on time. The first order term has an envelope with the same length as the third order bound wave $\eta_{sb}^{(3)*}(x,t)$. Thus superposition of the first order term with the third order side band bound and free waves leads to a spatial envelope with a short modulation length $\lambda_s = 4\pi/[|-\frac{1}{2}K''(\omega_0)\nu^2| + |(\overline{k^{nl}} - k_0^{nl})|]$ and a longer modulation length $\lambda_l = 4\pi/||-\frac{1}{2}K''(\omega_0)\nu^2| - |(\overline{k^{nl}} - k_0^{nl})||$. These values of λ_s and λ_l are obtained by only considering the superposition of the third order bound waves and free waves where λ_s shows how MTA oscillates with λ_l as the overall 'wave length' of the MTA. Furthermore, since the spatial envelopes of the third order bound waves and free waves contain the phase α, the location of the first maximal position of MTA can be expressed in the form

$$\begin{aligned}
\hat{x}_{\max} &= \frac{\pi}{|-\frac{1}{2}K''(\omega_0)\nu^2| + |(\overline{k^{nl}} - k_0^{nl})|} - \frac{2\alpha}{-\frac{1}{2}K''(\omega_0)\nu^2 + (\overline{k^{nl}} - k_0^{nl})} \\
&= \frac{\pi}{|-\frac{1}{2}K''(\omega_0)\nu^2| + |(k_1^{(2)} + k_3^{(2)})/2 - k_0^{(2)}|} - \\
&\quad \frac{2\alpha}{-\frac{1}{2}K''(\omega_0)\nu^2 + (k_1^{(2)} + k_3^{(2)})/2 - k_0^{(2)}} \\
&= \mathcal{O}\left(\frac{1}{\nu^2}, \frac{1}{a^{(2)}}\right),
\end{aligned} \tag{28}$$

where the expressions for $k_i^{(2)}$, $i = 1, 2$ and k_0^{nl} are described in the previous section.

4. Verification of the derived formulas

In what follows, we verify the formulas derived in Section 3. For the case of bi-chromatics signals, we use available numerical and experimental results. For the experiments, the propagated signals are measured only at a limited number of locations in the wave tank; hence, the location where the MTA is maximal, the extreme position, can only be obtained within a range determined by the locations where the signals are measured. For the case of BF signals, verifications are done through the exact expression of the physical SFB solution.

In this section we use laboratory variables in standard SI units [m,s]. We consider a typical wave tank with a layer of water of 5m deep, and with a length of 250m, and express all quantities in laboratory variables.

Table 1: Comparisons of the extreme positions: $\check{x}_{\max}$ calculated with third order theory (20) above, the numerical results $x_{\max(HBR)}$ calculated numerically, and the experimental result $x_{\max(EXP)}$ with specification of the various cases listed in the given references.

Case	$x_{\max(HBR)}$	$\check{x}_{\max}$	$x_{\max(EXP)}$
$q = 0.09, \omega_+ = 3.264, \omega_- = 3.028$	155.0m	157.50m	140m-160m, [20]
$q = 0.08, \omega_+ = 3.300, \omega_- = 2.990$	127.0m	118.00m	100m-120m, [18] & [20]
$q = 0.09, \omega_+ = 3.300, \omega_- = 2.990$	109.8m	110.90m	100m-120m, [20]
$q = 0.10, \omega_+ = 3.491, \omega_- = 2.856$	47.0m	48.62m	40m-60m, [20]

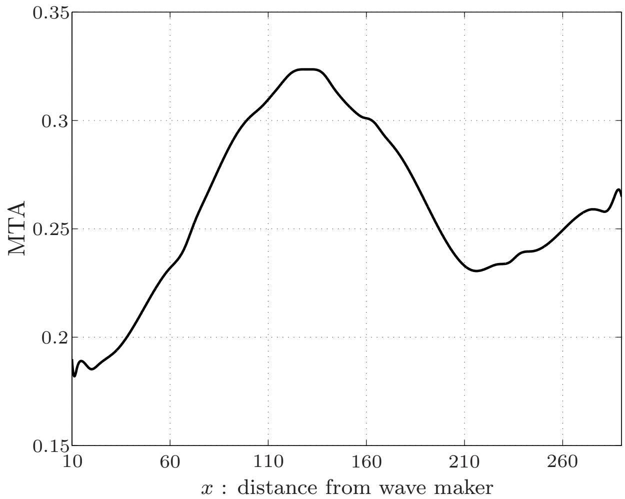

Figure 1: MTA for bi-chromatics signal with $q = 0.08$, $\omega_+ = 3.3$, $\omega_- = 2.99$ and $\nu = 0.155$.

4.1. Verification for bi-chromatics input signals

The predicted extreme position $\check{x}_{\max}$ derived by the third order approximation (TOA) in (20) will be compared with results from a numerical wave tank, HUBRIS, used at Maritime Research Institute Netherlands (MARIN) [20] and with experimental results reported in [18, 20]. We present the results in Table 1, providing the reference to the experiments. It is seen that the predicted values are reasonably close to both the numerical values as well as to the experimental results.

In Figure 1, we present MTA curve computed numerically with HUBRIS for an input bi-chromatics signals with amplitude $q = 0.08$, and frequencies of the mono-chromatics $\omega_+ = 3.30$ and $\omega_- = 2.99$. Experiments for this case have been conducted independently in [18] and [20] where in both experiments the largest signal appears at a distance of approximately 120m away from the wave-maker, which is the extreme position. In Figure 2, we show signals at different locations in the wave tank computed using HUBRIS. As

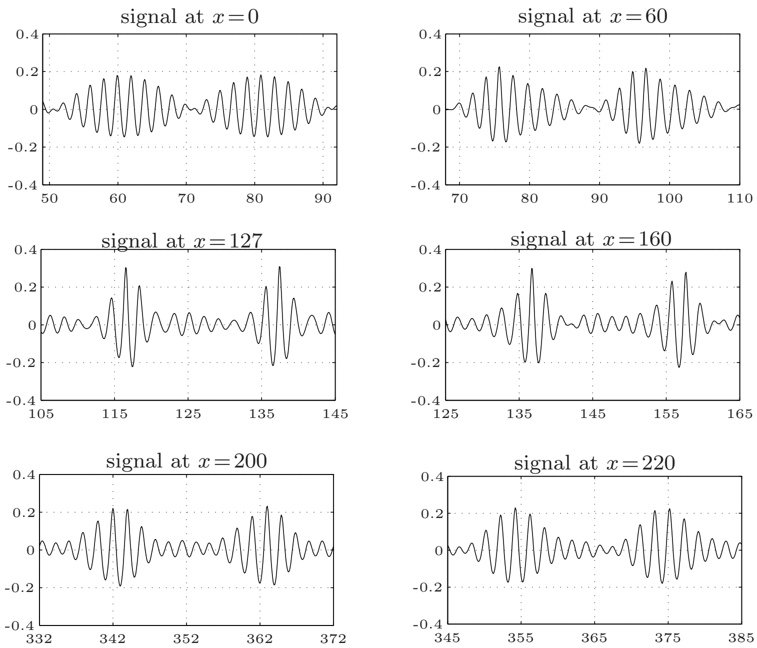

Figure 2: Bi-chromatics signal at some positions with $q = 0.08$, $\omega_+ = 3.30$, $\omega_- = 2.99$ and $\nu = 0.155$ computed using HUBRIS.

shown in Table 1, for this case the third order approximation in (20) gives the position of $\check{x}_{\max} \approx 118$m away from the wave-maker. This result of the extreme location shows a good agreement with the same approximation using multidirectional KP model for multidirectional wave in case the wave propagation angle is zero(see[14]).

4.2. Approximated MTA for BF input signals

In the next subsection we will verify the derived formula for the extreme position $\hat{x}_{\max}$ in (28) for an initial BF signal by comparing with an exact analytical solution SFB. Before doing so, in this subsection we will first show that the global behaviour of MTA can be captured by the first and third order terms only. Further we will illustrate that although we do not use all the third order terms in approximating this location $\hat{x}_{\max}$, the derived formula is reasonably good in comparison to first maximum $x_{\max}$ of $m_{-2}(x) = \max_t[\widetilde{\eta}(x,t) - \eta^{(2)}(x,t)]$, where $\widetilde{\eta}(x,t)$ contains all orders.

We take $a_0 = 0.16$m, $\delta = 0.1$, $\omega_0 = 3.145/s$ and $\nu = 0.155/s$ with some different values of α related to the phases of the mono-chromatic components. The non-linear coefficient of KdV is taken to be $\mu = 3/2$, see [8].

In Figure 3, we show MTA as a function of x based on the full third order solution. The upper figure shows $m(x) = \max_t \widetilde{\eta}(x,t)$ and the lower figure is obtained when the

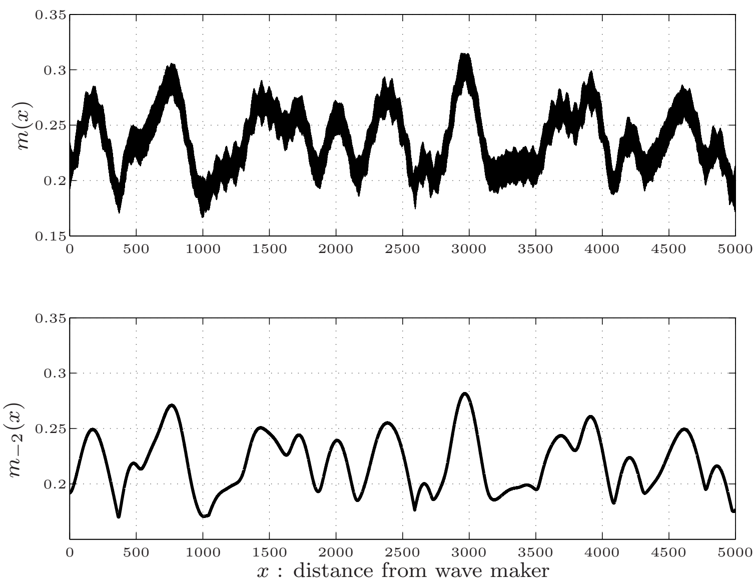

Figure 3: The Maximal Temporal Amplitude calculated in the upper figure with all orders, $\max_t \widetilde{\eta}(x,t)$, and in the lower figure without the second order contributions: $\max_t[\widetilde{\eta}(x,t) - \eta^{(2)}(x,t)]$.

Table 2: The first maximum $x_{\max}$ of $m_{-2}(x)$ and the approximated value $\hat{x}_{\max}$ in (28) for various values of phases α.

Case	$x_{\max}$ for $m_{-2}(x)$	$\hat{x}_{\max}$
$\alpha=\pi$	173.5m	185.06m
$\alpha=\pi/2$	343.0m	370.13m
$\alpha=\pi/3$	302.0m	308.40m
$\alpha=\pi/4$	280.0m	277.60m
$\alpha=\pi/5$	261.5m	259.10m
$\alpha=\pi/6$	246.5m	246.75m

second order terms are subtracted: $m_{-2}(x) = \max_t[\widetilde{\eta}(x,t) - \eta^{(2)}(x,t)]$. The phases of the tri-chromatics are $\psi_0 = 0$, $\alpha = \beta = 0$ so that $\psi_1 = \psi_3 = 0$. It is seen from these results that the global behaviour of the MTA $m(x)$ can be captured by the third order interaction $m_{-2}(x)$ only.

For the case above the first position of $m_{-2}(x)$ is $x_{\max} = 180$m while the approximate $\hat{x}_{\max} = 185$m. We will now investigate how the phases of the mono-chromatic components influence the value $x_{\max}$ and $\hat{x}_{\max}$. In Table 2, we show the value $x_{\max}$ and the predicted value $\hat{x}_{\max}$ for the same case above but for different values of α. In Figure 4 we show $m_{-2}(x)$ for two different values of α, the upper figure for $\alpha = 0$ and the lower one for

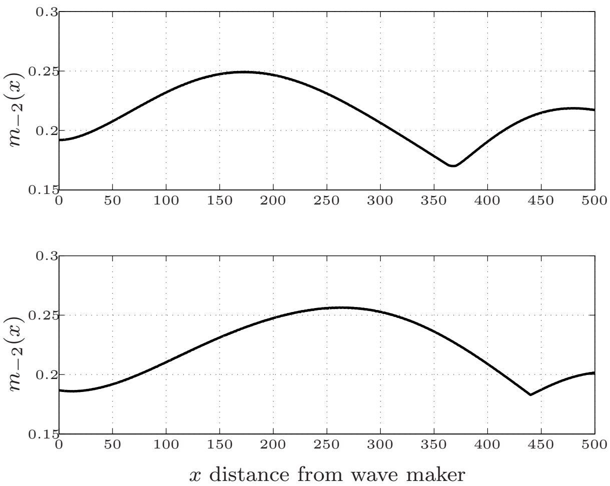

Figure 4: Maximal Temporal Amplitude for two different values of α, (Upper) α=0 and (lower) α=$\pi/4$.

$\alpha = \pi/4$. It is clearly seen that there is a significant difference of the location where the maximum value is obtained.

4.3. Comparison of MTA of SFB and third order calculations

Since numerical and experimental results are not easily accessible, to verify the derived formula (28) we use an exact solution SFB which is a special solution of NLS equation.

First we briefly describe this SFB solution. It is an exact solution of the spatial NLS equation that corresponds to the KdV equation. With $\eta(x,t)$ the wave elevation, we write $\eta(x,t)$ with a complex slowly varying envelope $A(\xi,\tau)$

$$\eta(x,t) = A(\xi,\tau)e^{i(k_0x-\omega_0t)} + c.c. \tag{29}$$

with slow variables $\xi = x$ and shifted time variable $\tau = t - x/\Omega'(k_0)$. Then this complex amplitude satisfies the spatial NLS equation that can be derived as in [8]. From [1] an exact solution called *soliton-on-finite-background* (SFB) can be found for this equation, which is a modulation of a mono-chromatic signal by a small frequency ν, explicitly given by

$$A(\xi,\tau) = \Lambda(\xi,\tau)a_0e^{ia_0^2\gamma\xi}, \tag{30}$$

where

$$\Lambda(\xi,\tau) = \frac{(\hat{\nu}^2-1)\cosh(\kappa\xi) + \sqrt{1-\hat{\nu}^2/2}\cos(\nu\tau) + i\hat{\nu}\sqrt{2-\hat{\nu}^2}\sinh(\kappa\xi)}{\cosh(\kappa\xi) - \sqrt{1-\hat{\nu}^2/2}\cos(\nu\tau)}.$$

Here $\widehat{\nu}$ is a normalised modulation frequency such that $0 < \widehat{\nu} < \sqrt{2}$ is the region of Benjamin Feir (BF) instability. The wavenumber κ is given by $\kappa(\nu) = \beta\nu\sqrt{2\nu_*^2 - \nu^2} =$

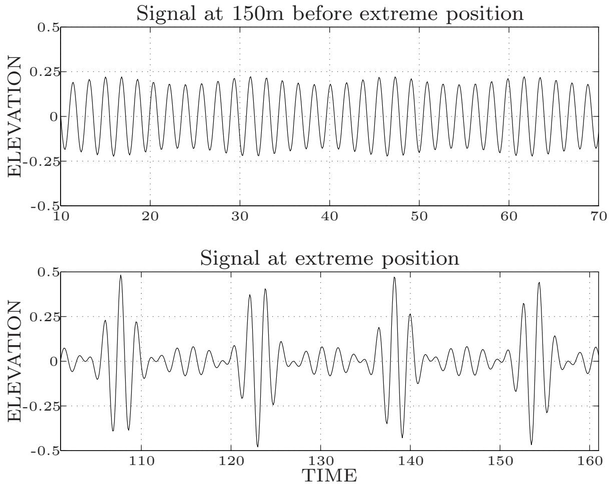

Figure 5: SFB signal with parameters $(\omega_0, a_0, \widehat{\nu}) = (3.5, 0.1, 1)$. (Upper) at 150m before extreme position and (lower) at extreme position.

$\gamma r_0^2 \hat{\nu}\sqrt{2-\hat{\nu}^2}$. The largest elevation is at $(\xi, \tau) = (0, 0)$ and at far distance from the position $\xi = 0$, $|A(\xi, \tau)| \to a_0$ for $\xi \to \pm\infty$. This shows that a_0 is the amplitude of the asymptotic monochromatic wave (the 'back ground'). Furthermore, it is seen that $1 < |A(\xi, \tau)|/a_0 < 3$ and $\lim_{\upsilon \to 0} |A(\xi, \tau)|/a_0 = 3$. Hence, the largest possible amplification factor is 3.

The MTA of the SFB $m\,(x) = \max_t\, \eta(x, t)$ is explicitly given (up to a spatial shift) by (see [4])

$$\left(\frac{m\,(x)}{2a_0}\right)^2 = 1 + \frac{2\hat{\nu}^2\sqrt{1-\hat{\nu}^2/2}}{\cosh(\sigma x) - \sqrt{1-\hat{\nu}^2/2}}.$$

We will now use this exact solution to validate the derived formula $\hat{x}_{\max}$ in (28). We note here that the analytic SFB has precisely one extreme position (symmetric around this position), while the third order solution will produce some quasi-periodic curve; so globally very different. Therefore comparison can only be made with the first hump of the third order calculation.

We first take a case of SFB with parameters $(\omega_0, a_0, \widehat{\nu}) = (3.5,\ 0.1, 1)$. For these parameters, we map the signal at extreme position $(x, t) = (0, 0)$ into the position $x = L_D$ in the tank, a distance $L_D = 150$m from the wave-maker. In Figure 5 we present the SFB signal at the extreme position and at the position of the wave-maker. With $\widehat{\eta}(\omega)$ the Fourier transform of the signal at the wave-maker, the absolute value of the amplitude spectrum $\sqrt{\widehat{\eta}(\omega)\widehat{\eta}^*(\omega)}$ is given in the upper plot of Figure 6. This shows that the signal at the wave-maker can well be approximated by a superposition of three mono-chromatics, with frequencies $(\omega_0, \omega_1, \omega_3) = (3.5, 3.0916, 3.9084)$. From the signal at the wave-maker the corresponding phases in radiant are given by $(\psi_0, \psi_1, \psi_3) = (-1.5708, 1.0308, 0.5777)$.

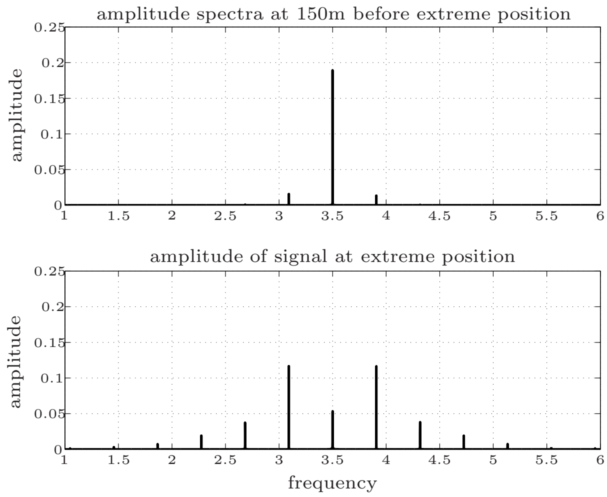

Figure 6: Amplitude spectra of SFB signal with parameters $(\omega_0, a_0, \widehat{\nu}) = (3.5,\ 0.1, 1)$. (Upper) at 150m before extreme position and (lower) at extreme position.

Table 3: Comparison of the extreme positions $\hat{x}_{\max}$ calculated with TOA (the third order approximation, given by (28)) and the exact value for the SFB solution, for various values of the parameters.

a_0	δ	ω_0	$\widehat{\upsilon}$	ψ_1	ψ_0	ψ_3	$m(0)$	$x_{max(\mathrm{SFB})}$	$\hat{x}_{\max}$
0.0822	0.146	3.7	0.70	−0.93	−1.82	−0.60	0.194	140m	145.6m
0.0849	0.120	3.7	0.80	−2.18	−1.79	0.54	0.196	140m	133.6m
0.0810	0.148	3.8	0.65	0.95	2.09	−0.87	0.190	130m	136.3m
0.0822	0.145	3.8	0.70	−2.88	−3.01	−1.03	0.194	125m	130.6m
0.0835	0.122	3.8	0.75	−0.47	2.12	0.46	0.192	130m	125.7m

The lower plot in Figure 6 is the amplitude spectrum at the extreme position, the position $x = 150$m in the wave tank.

Table 3 compares the position $\hat{x}_{\max}$ of the first maximum of the MTA approximated by the third order calculation (TOA) given by (28) with the position of the maximum MTA of the exact SFB. The results in Table 3 show that the predicted values are reasonably close to the exact values. To interpret the results of this table, we relate it to the significance of the MTA as illustrated in Figure 7. This picture shows a snap shot of wave elevation under the MTA curve for the SFB, which asymptotically looks like a slightly modulated monochromatic, corresponding to a BF signal. Shown is the spatial pattern: the modulated mono-chromatic evolves into wave-groups with largely deformed

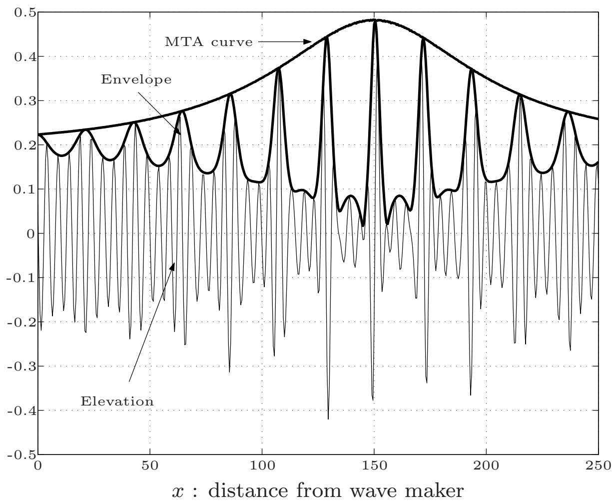

Figure 7: Snap shot of wave elevation under an MTA curve for a tri-chromatics signal based on SFB with parameters $(\omega_0, a_0, \widehat{\nu}) = (3.5,\, 0.1, 1)$.

envelopes, increasing in maximal amplitude till the extreme position $x_{\max(\mathrm{SFB})}$.

5. Concluding remarks

We have considered propagation in initially still water of waves generated at a wave-maker by a specific signal. The signals that were considered belong two classes of wave-groups, namely bi-chromatics and BF signals. Such signals can easily be used as input to a wave-maker at one side of a wave tank used in a hydrodynamic laboratory. The first class contains signals having two mono-chromatic components of the same amplitudes but slightly different frequencies. The BF signal is tri-chromatics: a mono-chromatic perturbed by two symmetric side bands. All these signals have a narrow banded spectrum. While propagating down stream from the wave-maker, the input signals changes in shape and amplitude; in the considered cases, a largely amplified elevation is found somewhere down stream in the tank. To find the precise location where the largest signal appears in the tank, the concept of MTA has been used. MTA gives at each location in the wave tank the maximum of the surface elevation over time. For deterministic extreme wave generation knowing this extreme position is of most interest. Furthermore, prescribing the position where the extreme wave has to appear in the wave tank, the MTA can be used to assist what kind of signal has to be generated at the wave-maker in such a way that the propagating signal produces the requested extreme wave elevation at the requested position.

For the two classes of wave-groups as input signals at the wave-maker, we have derived an approximation for the extreme position, using third order perturbation theory. We have investigated the effects of the phases of the mono-chromatic components on the location of the extreme position. We showed that for bi-chromatics signals, the location of maximum MTA is almost independent on the phases. For the BF signal, however, the phases of the mono-chromatic components influence the location of the maximum MTA considerably.

For the bi-chromatics case, we verified the calculated extreme position with published numerical and experimental results. Since experimental results for BF signals are not easily accessible we verified the formula using an exact solution of NLS equation called spatial Soliton on Finite Background which is a non-linear extension of the Benjamin Feir instablity. These comparisons show reasonably close values of the predicted locations and the known results. Thus we conclude that for a given input to the wave-maker in the form of bi-chromatics or BF signals the derived explicit formula can be used to predict the location where the most extreme wave elevations appear in the wave tank. Future works will focus on multi-directional wave propagation and apply similar methods used in this paper.

Acknowledgements

The authors are very grateful to Prof. E. van Groesen and Dr. Andonowati for fruitful discussion throughout the execution of this research. They sincerely thank Dr. Rene Huijsmans from Maritime Research Institute Netherlands and Dr. J. H. Westhuis for making HUBRIS accessible to verify the results of this paper.

References

[1] N. N. Akhmediev and A. Ankiewicz, Solitons-Nonlinear Pulses and Beams, Chapmann & Hall, 1997.

[2] Andonowati and E. van Groesen, *Optical pulse deformation in second order non-linear media*, Journal of Non-linear Optics Physics and Materials, vol. 12, no. 22, 2003.

[3] Andonowati, Marwan, E. van Groesen, *Maximal Temporal Amplitude of generated wave group with two or three frequencies*, Proc. of 2nd ICPMR&DT, Singapore, **v2**, 111–116, 2003.

[4] Andonowati, N. Karjanto, E. van Groesen, *Extreme waves arising from down stream evolution of modulated wave dislocation and non-linear amplitude amplification for extreme fluid surface waves*, Submitted to Mathematical Models and Methods in Applied Sciences, 2004.

[5] T. B. Benjamin and J. E. Feir, *The disintegration of wave trains on deep water. Part 1. Theory*, J. Fluid Mech., 27: 417, 1967.

[6] E. Cahyono, Analytical wave codes for predicting surface waves in a laboratory basin, Ph.D Thesis, Fac. of Mathematical Sciences Univ. of Twente, the Netherlands, 2002.

[7] M. A. Donelan and W. H. Hui, *Mechanics of ocean surface waves. Surface Waves and Fluxes*, Kluwer, Editors: G. L. Geernaert and W. J. Plants, **1**(1990), 209–246.

[8] E. van Groesen, *Wave groups in uni-directional surface wave models*, Journal of Engineering Mathematics, **34**(1998), 215–226.

[9] E. van Groesen, Andonowati and E. Soewono, *Non-linear effects in bi-chromatic surface waves*, Proc. Estonian Acad. Sci., Mathematics and Physics **48**(1999), 206–229.

[10] E. van Groesen, Andonowati and N. Karjanto, *Deterministic aspects of non linear modulation instability*, Proc. of Rogue Waves, Brest, France, 2004.

[11] R. Huijsmans, N. Karjanto, Andonowati, G. Klopman and E. van Groesen, *Extreme wave generation in* MARIN *wave tank: Part 1: Deterministic waves based on Soliton of Finite background*, Proc. of Rogue Waves, Brest, France, 2004.

[12] Longuet and M. S. Higgins, *Statistical properties of wave groups in a random sea state*, Philos. Trans. Roy. Soc. London, **A312**(1984), 219–250.

[13] Marwan and Andonowati, *Wave deformation on the propagation of bi-chromatics signal and its effect to the maximum amplitude*, JMS FMIPA ITB, **8**(2003), 81–87.

[14] Marwan, Toto Nusantara and Andonowati, *Spatial evolution of multidirectional surface gravity waves based on third order solution of KP equations*, Journal of Indones. Math. Soc., **12**(2006), 211–224.

[15] A.R. Orsbone, M. Onorato and M. Serio, *The nonlinear dynamics of rogue waves and holes in deep water gravity wave trains*, Physics Letters A, **275** (2000), 386–393.

[16] A. R. Orsbone, *The random and deterministics dynamics of rogue waves in unidirectional, deep water wave trains*, Marine Structures **14**, 275–293.

[17] O. M. Phillips, D. Gu and M. A. Donelan, *Expected structure of extreme waves in a Gaussian sea. Part I. Theory and SWADE buoy measurements*, J. Phys. Oceanogr **23**(1993), 992–1000.

[18] C. T. Stansberg, *On the non–linear behaviour of ocean wave groups*, Ocean Wave Measurement and Analysis, Reston, VA, USA : American Society of Civil Engineers (ASCE), Editors: B. L. Edge and J. M. Hemsley, **2**(1998), 1227–1241.

[19] J. Westhuis, E. van Groesen and R. H. M. Huijsmans, *Long time evolution of unstable bi-chromatic waves*, Proc. 15th IWWW & FB, Caesarea Israel (2000), 184–187.

[20] J. Westhuis, E. van Groesen and R. H. M. Huijsmans, *Experiments and numerics of bi-chromatic wave groups*, J. Waterway, Port, Coastal and Ocean Engineering, **127** (2001), 334–342.

[21] G. B. Whitham, Linear and Non-Linear Waves, John Wiley and Sons, New York, 1974.

Department of Mathematics, Faculty of Science, Syiah Kuala University, Banda Aceh-Indonesia.
E-mail: marwan.ramli@math-usk.org